AJNR

Direct Oblique Sagittal CT of Orbital Wall Fractures

James B. Bali, Jr.

AJNR Am J Neuroradiol 1987, 8 (1) 147-154
http://www.ajnr.org/content/8/1/147

Direct Oblique Sagittal CT of Orbital Wall Fractures

James B. Ball, Jr.[1]

Direct oblique sagittal CT was used to evaluate trauma to 77 orbits. Sixty-seven orbital wall fractures with intact orbital rims (36 floor, 22 medial wall, nine roof) were identified in 47 orbits. Since persistent diplopia and/or enophthalmos may warrant surgical repair of orbital floor fractures, optimal imaging should include an evaluation of extraocular muscle status, the nature and amount of displaced orbital contents, and an accurate definition of fracture margins. For orbital floor fractures, a combination of the direct oblique sagittal and direct coronal projections optimally displayed all fracture margins, the fracture's relationship to the inferior orbital rim and medial orbital wall, and the amount of displacement into the maxillary sinus. Inferior rectus muscle status with 36 floor fractures was best seen on the direct oblique sagittal projection in 30 fractures (83.3%) and was equally well seen on sagittal and coronal projections in two fractures (5.5%). Floor fractures were missed on 100% of axial, 5.5% of sagittal, and 0% of coronal projections. Since the direct oblique sagittal projection complements the direct coronal projection in evaluating orbital floor fractures, it should not be performed alone. A technical approach to the CT evaluation or orbital wall fractures is presented.

Fracture of the orbital floor was first described in 1844 [1], and a case of traumatic enophthalmos was reported 45 years later [2]. The term "blow-out fracture" of the orbital floor was coined by Smith and Regan [3]. Orbital floor blow-out fractures are the third most common fracture of the middle third of the face [4]. The reported incidence of medial orbital wall fractures in association with orbital floor fractures is 5–71%, while isolated medial orbital wall fractures are said to be uncommon [5, 6]. Fractures of the orbital roof are unusual, normally occurring into the floor of the frontal sinus [7].

The use of both axial and coronal CT projections is well established. Our technique for obtaining direct sagittal images of the cranium and face was recently described [8].

The purpose of this study is to assess the usefulness of direct oblique sagittal CT of the orbit in evaluating orbital wall fractures and to determine the optimal CT technique for evalulating suspected orbital wall fractures.

Materials and Methods

During an 18-month period, 74 patients were referred for CT to evaluate the presence and extent of orbital trauma. In three patients evaluation of both orbits was requested, for a total of 77 orbits (36 left, 41 right). There were 20 women and 54 men, ranging in age from 16 to 64 years (mean, 31.9).

CT examinations of all 74 patients were performed on a GE 9800 scanner. All 77 orbits were evaluated in the oblique sagittal plane using a technique previously described [8]; three examinations used contiguous 5-mm slices and the rest used contiguous 3-mm slices. Seventy-three orbits were also evaluated in the coronal plane; six examinations used contiguous 3-mm slices and the rest used contiguous 5-mm slices. Six orbits were examined in the axial plane; two examinations used contiguous 5-mm slices and four examinations

This article appears in the January/February 1987 issue of *AJNR* and the March 1987 issue of *AJR*.

Received January 22, 1986; accepted after revision May 27, 1986.

Presented at the annual meeting of the American Society of Neuroradiology, San Diego, January 1986

[1] Department of Radiology, Division of Neuroradiology, University of Cincinnati Medical Center and University Hospitals, Cincinnati, OH 45267-0742. Present address: Florida Hospital, 601 E. Rollins, Orlando, FL 32803. Address reprint requests to J. B. Ball.

***AJNR* 8:147–154, January/February 1987**
0195–6108/87/0801–0147

used contiguous 3-mm slices. Seventy-one orbits were evaluated in both sagittal and coronal planes. Four orbits were evaluated in both sagittal and axial planes. Two orbits were evaluated in all three planes.

When available, a retrospective review was made of the patient's chart for clinical data. All CT examinations were reviewed retrospectively.

To assess the relative radiation dose to the lens using these three CT planes, a tissue-equivalent head phantom was scanned with thermoluminescent dosimeters (TLDs) placed on the lens. For each of the three planes (axial, coronal, sagittal), two slice widths were used (contiguous 3-mm and contiguous 5-mm) for a total of six techniques. In the coronal technique, the neck was hyperextended. Eight slices per technique were used to scan through the lens. Technical factors were: 120 kV, 200 mA, 3 sec. A scout view preceded each technique (120 kV, 100 mA). Six TLDs per technique were used and these results were averaged. A background determination was made from four TLDs.

Results

Clinical data are available for 64 orbits. Two patients had exophthalmos, both with floor fractures. Four patients had enophthalmos, three with floor fractures and one with a tripod fracture. Thirteen patients had diplopia, six with floor fractures, three with a tripod fracture, one with a roof fracture, and three with no visible fracture. Sixteen patients had limitation of eye movement, 12 with floor fractures, two with a tripod fracture, one with a roof fracture, and one with both a tripod and roof fracture.

Sixty-seven orbital wall fractures were identified in 47 orbits. Thirty-six (54%) involved the orbital floor, 22 (33%) involved the medial orbital wall, and nine (13%) involved the orbital roof. Twenty-seven (57%) of the 47 orbits had only one wall fractured.

For the 36 orbital floor fractures, distance from the inferior orbital rim to the fracture site (average 7.8 mm, range 2–22 mm) and depth of fracture (average 19.5 mm, range 2–30 mm) were measured on sagittal images; width of fracture (average 16.2 mm, range 5–30 mm) was measured on coronal images; and inferior displacement of fracture fragments (average 6.3 mm, range 0–11 mm) was measured on whichever projection showed the greatest displacement. Thickening and/or displacement of the muscle toward the fracture site was seen with the inferior rectus muscle in 22 (61%) and with the medial rectus muscle in seven (19%). Thickened muscles represent edema and/or hemorrhage. Entrapment by bony fragments was not identified.

The projection best demonstrating the pathologic findings associated with 36 orbital floor fractures is shown in Table 1. While inferior rectus muscle status was best determined on the sagittal projection, muscle thickening was frequently easier to appreciate on the coronal projection where the opposite inferior rectus muscle was available for comparison.

Two (5.5%) of the 36 floor fractures were not identified in the sagittal plane. Neither of the two floor fractures scanned in the axial plane was identified in this plane. All 34 floor fractures scanned in the coronal plane were identified in this plane.

Other fractures identified included 12 zygomaticomaxillary (tripod), 10 anterior maxillary sinus wall, and five inferior orbital rim/anterior maxillary sinus wall. Twelve orbits demonstrated no fracture. Associated with the nine orbital roof fractures were one frontal lobe hematoma, one squamous frontal epidural hematoma, one subfrontal epidural hematoma, one superior rectus muscle impingement, and one greater sphenoid wing fracture.

Radiation dose to the lens as determined by phantom scanning with TLDs is shown in Table 2. Radiation dose to the four control TLD chips was negligible.

Discussion

The term "blow-out fracture" [3] is best reserved for orbital wall fractures with intact adjacent orbital rims. Sixty-seven orbital wall blow-out fractures occurred in 47 of 77 orbits studied for orbit trauma, including 36 orbital floor, 22 medial orbital wall, and nine orbital roof fractures.

There are two proposed mechanisms for the production of orbital wall blow-out fractures. The most commonly accepted mechanism is a sudden increase in intraorbital hydraulic pressure due to force delivered to the anterior globe by an object

TABLE 2: **Radiation Dose to the Lens with Thermoluminescent Dosimeters**

Projection	Slice Width (mm)	Average Dose (rad)
Sagittal	3	2.62
Sagittal	5	2.52
Axial	3	4.50
Axial	5	4.04
Coronal	3	5.99
Coronal	5	5.87

TABLE 1: **Projection(s) Best Demonstrating CT Findings in Orbital Floor Fractures**

Finding	No. of Fractures (%) (n = 36)				
	Not Involved	Sagittal and Coronal Equivalent	Sagittal	Coronal	Axial
Floor fracture	0	21 (58)	7 (19)	8 (22)	0
Contiguous medial wall involvement	27 (75)	1 (3)	1 (3)	6 (17)	1 (3)
Inferior rectus muscle status	0	2 (6)	30 (83)	4 (11)	0
Medial rectus muscle status	0	0	0	34 (94)	2 (6)

larger than the orbital rim, resulting in decompression of the orbit contents through the weakest portion of the orbital wall [9]. This mechanism would explain blow-out fractures of the orbital floor, medial wall, and roof. A second proposed mechanism for orbital floor blow-out fractures is floor buckling due to a force applied to the inferior orbital rim [10].

The need for and timing of surgical treatment of orbital floor fractures is controversial [3, 11, 12]. Most would agree that elective surgical treatment is best reserved for patients with persistent diplopia and/or enophthalmos [11]. Surgical treatment for medial orbital wall fractures is less common, and the same considerations of diplopia and enophthalmos apply. Surgical treatment of orbital roof fractures is usually dictated by other complications [13].

Since the sagittal plane is poor for evaluating medial orbital wall fractures, only orbital floor and roof fractures are discussed.

Orbital Floor Blow-out Fractures

Clinical findings with orbital floor fractures include periorbital ecchymosis, infraorbital hypesthesia, depression of the globe, exophthalmos, enophthalmos, decreased or absent extraocular muscle movement, and vertical diplopia [9, 14]. The most important late complications of missed orbital floor fractures are diplopia and enophthalmos [15].

Diplopia is common and usually resolves [11]. It may result from edema, hemorrhage, or damage to the nerve supply of the inferior rectus muscle. Diplopia from decreased mobility of the inferior rectus muscle may also occur by two other mechanisms [16]. Incarceration of the inferior rectus muscle by fracture fragments is a rare cause of diplopia and was not identified in this study. A more common cause is a restriction of inferior rectus muscle movement associated with herniation of the posterior inferior orbital fat pad through the fracture site into the upper maxillary sinus (Fig. 1). The posterior inferior orbital fat pad, lying between the orbital floor periosteum and the inferior rectus and inferior oblique muscles, has numerous fibrous connective tissue strands between the periosteum and the extraocular muscle sheaths. This is a vascular area with a large venular network draining into the inferior ophthalmic vein. Displacement of the posterior inferior orbital fat pad inferiorly with associated hemorrhage and edema within the fat pad causes increased tension on the fibrous strands between the floor periosteum and the inferior rectus muscle, resulting in a limitation of mobility [11, 12, 16]. Fibrosis within this "inferior rectus motility apparatus" may cause persistent diplopia after resolution of hemorrhage and edema [12]. Another proposed mechanism for chronic decreased mobility of the inferior rectus muscle after a relatively nondisplaced fracture is Volkmann's ischemic contracture [17]. Displacement of the globe below the visual axis will also result in diplopia [9, 18].

Enophthalmos may occur early or late [19]. Early enophthalmos is usually caused by disruption of the orbital floor periosteum with herniation of orbital contents into the maxillary sinus (Fig. 1) or displacement of the orbital floor inferiorly resulting in an increase in intraorbital volume despite an intact periosteum (Fig. 2). Late enophthalmos may result from orbital fat atrophy and/or fibrotic contraction of extraocular muscles due to injury. The incidence of enophthalmos is 8–54% within weeks to months after injury [20]. Enophthalmos may be masked early because of traumatic hemorrhage and edema [15, 19]. A large fracture volume may suggest the need for early surgical repair to prevent enophthalmos [21]. A positive correlation of fracture area with enophthalmos has been reported.

CT can evaluate both bony and soft-tissue components of the orbit. Its optimal use depends on an understanding of the pertinent anatomy of the orbital floor and adjacent soft-tissue structures. The orbits are roughly conical with their long axes diverging about 45° from the midsagittal plane. The long axes of the optic nerve and inferior rectus muscle deviate about 30–35° from the midsagittal plane.

The orbital floor slopes downward from posterior to anterior and from medial to lateral (Fig. 3), with an undulating contour

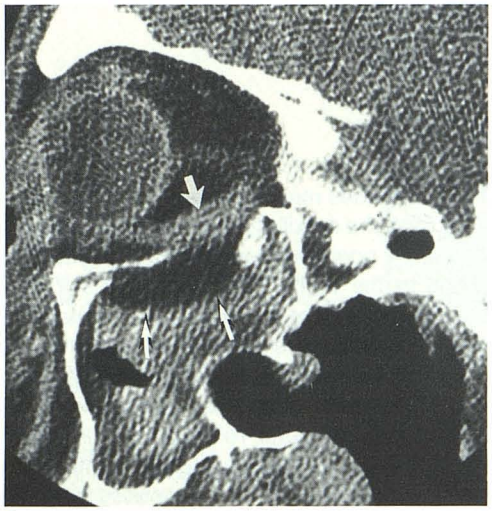

Fig. 1.—Floor fracture and acute enophthalmos explained on direct oblique sagittal projection by herniation of posterior inferior orbital fat pad (*small arrows*) into maxillary sinus associated with thickening and displacement of inferior rectus muscle (*large arrow*). Note optimal longitudinal imaging of inferior rectus muscle.

1

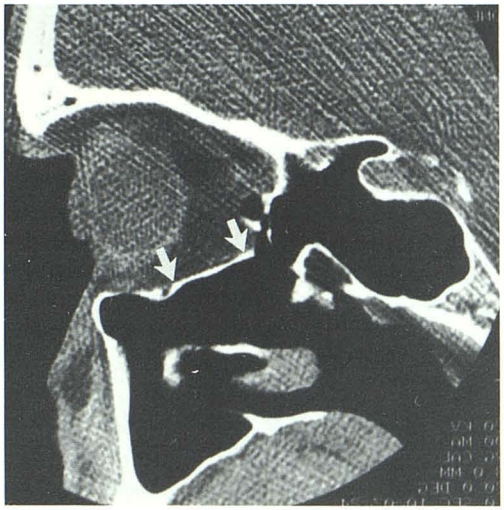

Fig. 2.—Floor fracture and acute enophthalmos caused by inferior displacement of orbital floor (*arrows*) with resultant increase in intraorbital volume.

2

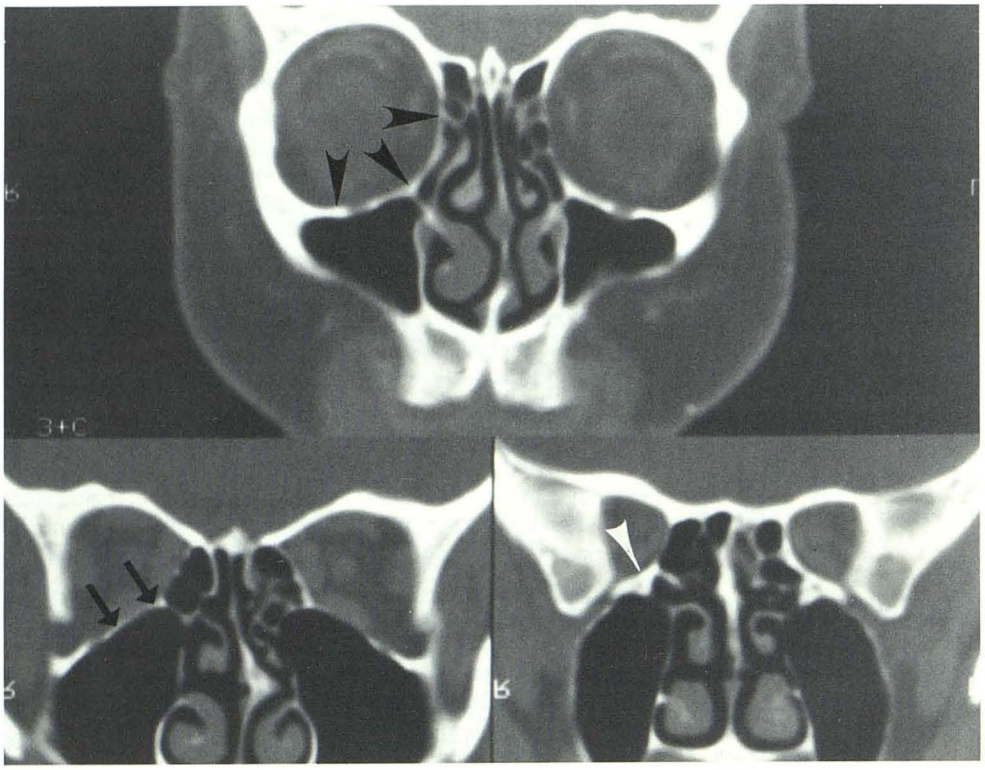

Fig. 3.—Curving junction of orbital medial wall and floor with downward sloping of floor just posterior to orbital rim (*black arrowheads*), about halfway between orbital rim and apex (*arrows*), and just anterior to apex (*white arrowhead*).

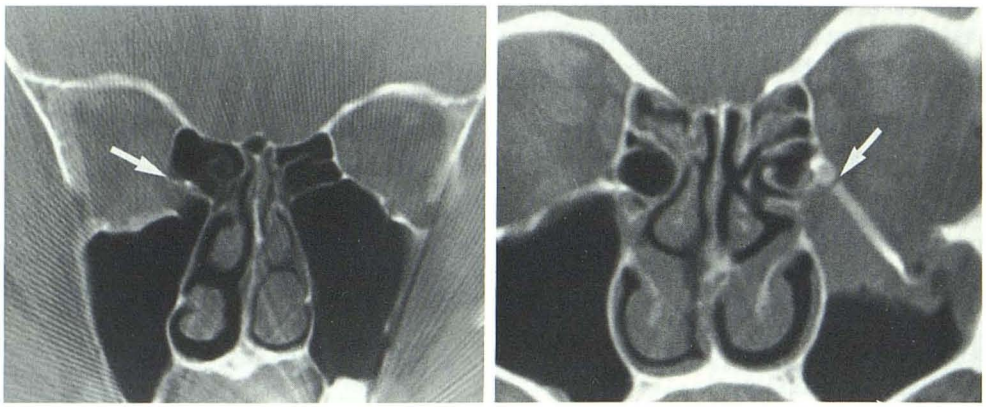

A B

Fig. 4.—Different patients with medial margin of floor fracture at or near maxillary-ethmoid plate (*arrows*), hinged laterally (*A*) and medially (*B*).

that is superiorly convex posteromedially. The thinnest portion of the orbital floor is the floor of the infraorbital groove posteriorly. The next thinnest portion is medial to the infraorbital groove just anterior to the inferior orbital fissure. This is the most common site of orbital floor fracture. The thickest portion of the orbital floor lies lateral to the infraorbital groove and anterior to the inferior orbital fissure [22]. The orbital floor has no well-defined boundaries, forming a curving junction with the medial orbital wall (Fig. 3). It is generally defined by the limits of the maxillary sinus roof, and thus a fracture crossing the maxillary-ethmoid plate also involves the contiguous medial orbital wall. Of the 27 orbital floor fractures that did not involve the contiguous medial orbital wall, most had a medial margin at or near the maxillary-ethmoid plate (Fig. 4).

Depending on patient positioning and gantry angle, axial CT is nearly parallel to the orbital floor and is thus a poor method for evaluating orbital floor fractures. Both orbital floor fractures scanned in the axial plane in this study were missed with contiguous 3-mm images on this projection. The only advantage of axial CT is the ease of patient positioning. While thin-section axial CT with computer reformations has been advocated [16], the resulting spatial resolution is inferior to that of direct coronal or sagittal CT.

Since direct coronal CT is nearly perpendicular to all four

orbital walls, it is the best projection for evaluating trauma to the middle third of the face and orbits. No orbital floor fracture was missed on the coronal projection in 34 cases in this study. It is the best projection for evaluating the medial and lateral extent of floor fractures and for assessing inferior rectus muscle size since comparison with the contralateral side is possible (Fig. 5A). However, the anterior and posterior limits of the fracture are not optimally demonstrated in the coronal plane, and coronal images are not optimal for evaluating displacement of the inferior rectus muscle (Fig. 6) because of poor definition of muscle kinks [16].

With the patient supine and the neck hyperextended it is rare that the gantry can be tilted enough to make the coronal plane directly perpendicular to the orbital floor. An alternative method of patient positioning is supine with the neck hyperflexed [23]. In most patients this will allow the coronal plane to be directly perpendicular to the orbital floor, and thus it is probably the preferred method for performing direct coronal CT of the orbital floor. There is some increase in image noise and decrease in lens radiation dose because of inclusion of parts of the neck and shoulders in the scanning plane.

I agree with the suggestion of Hammerschlag et al. [16] that oblique sagittal sections be obtained through the plane of the inferior rectus muscle for optimal evaluation of orbital floor fractures. Their method, however, was to perform axial CT with computer reformations. Our method of obtaining direct oblique sagittal CT images of the orbital floor [8] results in superior spatial resolution. For scanning the orbit with this technique, the orbit of interest is placed away from the positioning block and the patient's head turned about 30° toward the positioning block (Fig. 7A) so that the scanning plane is parallel to the course of the optic nerve and inferior rectus muscle. Using the lateral scout view, a gantry angle is chosen that does not pass directly through the vertical plane of the orbit, but rather runs slightly superolateral to inferomedial so that the scan plane is more nearly perpendicular to the laterally sloping orbital floor (Fig. 7B).

The main advantage of this direct oblique sagittal plane is longitudinal imaging of the inferior rectus muscle in one or two CT sections so that the course of the inferior rectus muscle is better appreciated (Figs. 1 and 6B). In our study, inferior rectus muscle status was demonstrated best on the

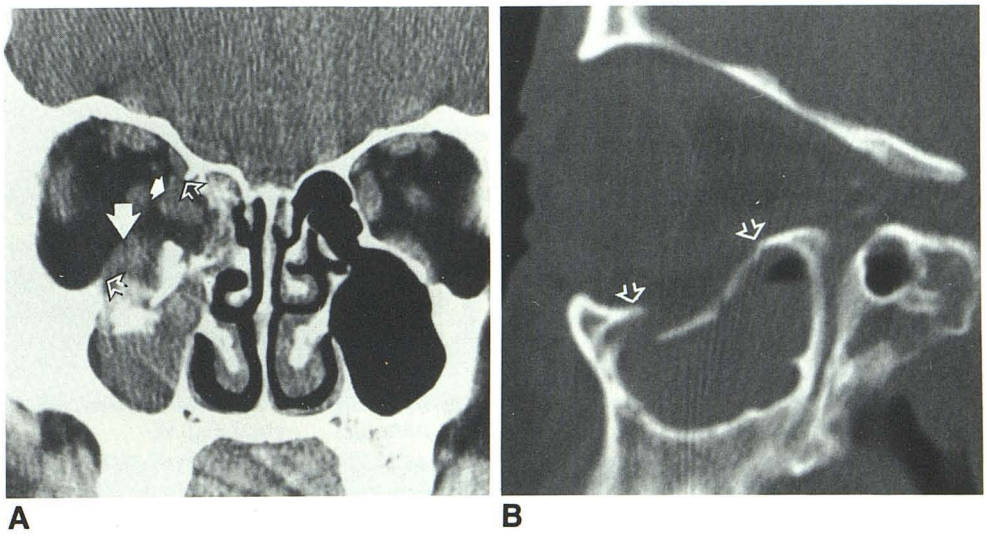

Fig. 5.—Floor fracture with contiguous medial-wall involvement best evaluated with combination of coronal (*A*) and direct oblique sagittal (*B*) projections. This combination accurately defines all fracture margins (*open arrows*). Coronal projection is best for demonstrating medial-wall involvement and is perpendicular to long axes of medial (*small white arrow*) and inferior (*large white arrow*) rectus muscles, allowing size comparison with contralateral side.

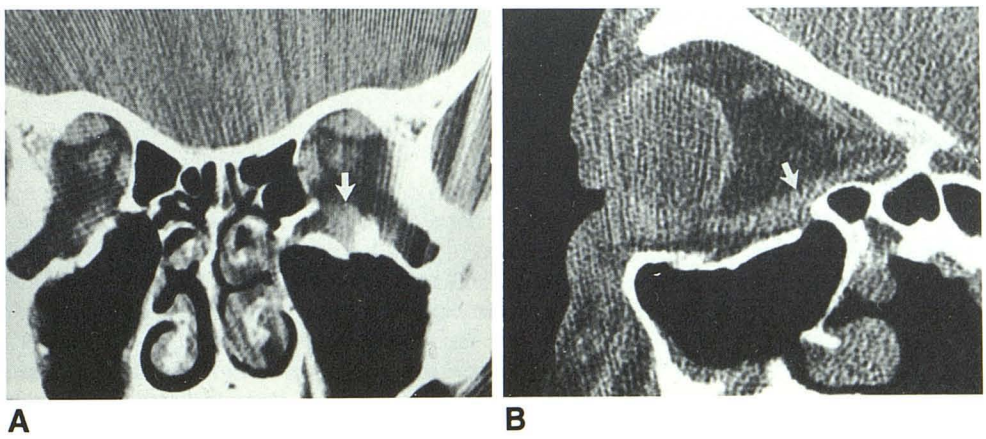

Fig. 6.—Floor fracture with inferior rectus muscle status best demonstrated on direct oblique sagittal projection. While coronal projection (*A*) demonstrates thickening and some displacement of inferior rectus muscle (*arrow*), exact relationship to fracture site is uncertain. Direct oblique sagittal projection (*B*) allows optimal longitudinal imaging of inferior rectus muscle (*arrow*), demonstrating relationship to posterior fracture margin.

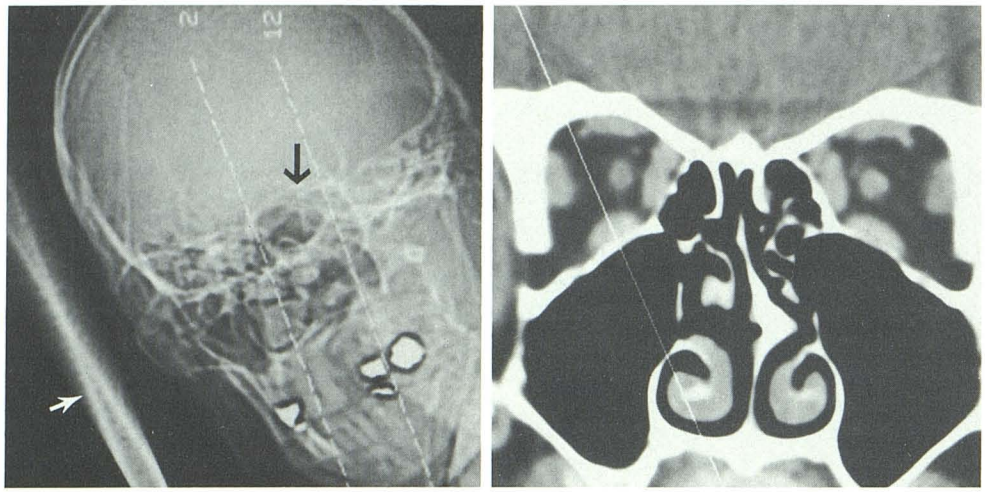

A B

Fig. 7.—*A* and *B*, Direct oblique sagittal technique: Patient prone on scanner table (not shown) with neck flexed laterally and head placed against surface of positioning block (*white arrow*) so that orbit of interest (*black arrow*) is away from positioning block. Head turned about 30° toward positioning block so that scan plane is parallel to long axis of orbit of interest and inferior rectus muscle. Gantry angled so that scan plane is perpendicular to downward-sloping orbit floor (*white lines*), not parallel to vertical plane of orbit.

sagittal projection in 83% of floor fractures, and the sagittal and coronal projections were equivalent in 6%. The precise relationship of the anterior fracture margin to the inferior orbital rim as well as to the anterior and posterior margins of the floor fracture are also best determined with the direct oblique sagittal plane (Fig. 5B).

Disadvantages of the direct oblique sagittal technique include difficulty in patient positioning, requiring better technical assistance; suboptimal evaluation of involvement of the medial orbital wall, either contiguously or with a separate blow-out fracture; and no demonstration of the contralateral orbit, and thus suboptimal evaluation of other midface fractures. As with the coronal plane, artifacts from dental fillings can be a problem.

Direct oblique sagittal CT should be a supplement to, not a replacement for, the direct coronal projection. Two (5.5%) of 36 orbital floor blow-out fractures in our study were not identified on the direct oblique sagittal projection. Although the orbital floor was not clearly normal in either case, a definite fracture was not identified. These were small, relatively nondisplaced fractures.

The optimal CT technique for evaluating orbital floor blow-out fractures includes two projections: the direct coronal projection with the patient supine and neck hyperflexed and the direct oblique sagittal projection (Figs. 5 and 6).

Orbital Roof Fractures

The clinical setting in which orbital roof fractures occur is often different from that of orbital medial wall or floor fractures in that more significant trauma has usually occurred resulting in multiple and complex facial fractures. While diplopia and enophthalmos may occur, other more immediate clinical problems may take precedence.

Orbital roof fractures may result in ocular complications; structural deformity of the orbit; enophthalmos; extraocular muscle imbalance from superior rectus dysfunction; blepharoptosis from levator palpebrae injury; or intracranial complications including cerebrospinal fluid rhinorrhea, dural fistula, intracranial gas associated with dural tear, and meningitis [13].

Restriction of upward gaze caused by involvement of the superior rectus muscle results from mechanical impingement rather than entrapment [13]. In the presence of orbital floor fracture, the inability to elevate the globe may be from superior rectus injury accompanying associated orbital roof fracture [14] (Fig. 8).

As with orbital floor and medial wall fractures, evaluation of orbital soft-tissue structures is best performed with CT. CT is also suited to evaluation of the acute intracranial complications that often accompany orbital roof fractures. Three of our nine patients with orbital roof fractures had unsuspected intracranial hematomas, one intracerebral and two extracerebral (Fig. 9).

The direct coronal CT projection with the patient supine and neck hyperextended is nearly perpendicular to the orbital roof and is the best projection for evaluating orbital roof fractures (Fig. 9). It will also allow evaluation of the supraadjacent cranial compartment and may lead to detection of unsuspected hematomas. As with evaluation of the medial and inferior rectus muscles, the superior rectus muscle can be easily evaluated but is not optimally displayed in the coronal plane.

Direct oblique sagittal CT is the best method for evaluating the status of the superior rectus muscle (Fig. 8), which deviates from the midsagittal plane of the head in the same manner as the optic nerve and inferior rectus muscle. Because of the multiple convolutions of the orbital roof and increased image noise from scanning through the patient's neck and shoulder, small, relatively nondisplaced fractures are not easily seen on the sagittal projection.

The optimal CT technique for evaluating orbital roof fractures includes two projections, the direct coronal projection

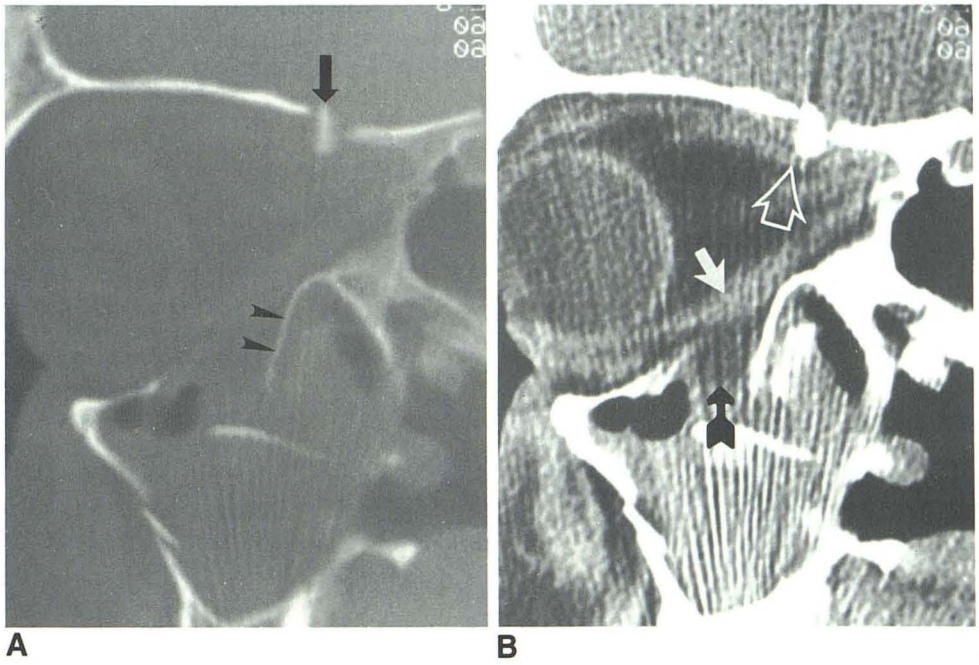

Fig. 8.—Direct oblique sagittal projection is optimal for evaluation of superior and inferior rectus muscles. Patient with limitation of eye movement on upward gaze after trauma.

A, Bone settings demonstrate floor fracture (*arrowheads*) and roof fracture with rotated fragment (*arrow*).

B, Soft-tissue settings demonstrate nondisplaced inferior rectus muscle (*white arrow*) with some fat herniation into maxillary sinus (*black arrow*) associated with floor fracture. Eye movement is limited, however, because of impingement of roof-fracture fragment on superior rectus muscle complex (*open arrow*).

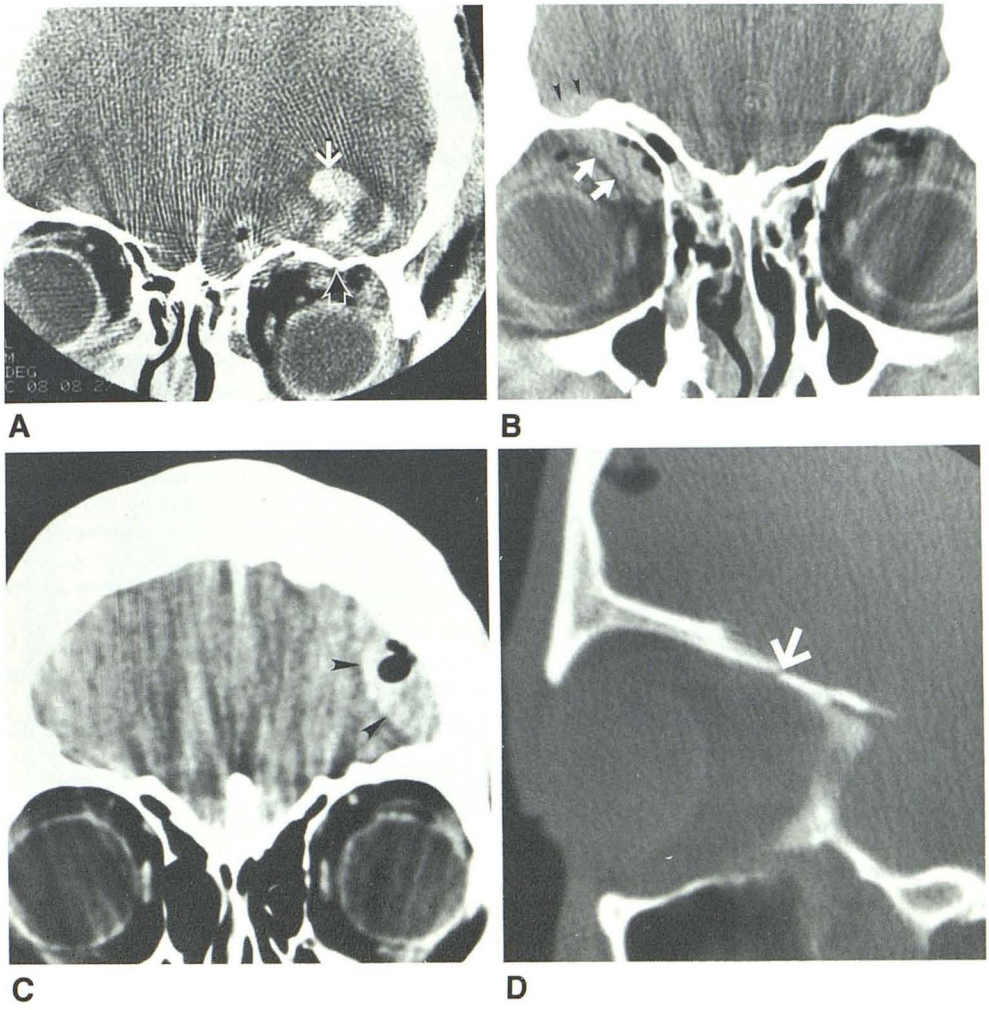

Fig. 9.—Intracranial hematomas associated with orbital roof fractures.

A, patient with intracerebral hematoma (*closed arrow*) associated with roof fracture (*open arrow*).

B, Patient with subfrontal epidural hematoma (*arrowheads*) as well as intraorbital hematoma (*arrows*) associated with orbital roof fracture (not shown).

C and *D*, Patient with gas-containing epidural hematoma (*arrowheads*) associated with roof fracture (*arrow*).

with the patient supine and neck hyperextended (Fig. 9A) and the direct oblique sagittal projection (Fig. 8).

Radiation Considerations

The greatest radiation dose to the lens in our phantom determinations (Table 2) was with the coronal hyperextended projection, because there is little other body tissue in the scanning plane. In practice it is not always necessary to scan directly through the lens while including the entire orbital floor. Using the hyperflexed neck technique will also decrease lens radiation dose because of inclusion of the neck and shoulders in the scanning plane. For the same reason (inclusion of neck and shoulders in the scanning plane), the least lens radiation dose in our phantom determinations was with the sagittal projection. The increased dose with thinner slices was minimal. The small additional lens radiation exposure from using the sagittal projection should not deter its use, especially when combined with the coronal projection with neck hyperflexed and the lens excluded from the coronal scans.

In conclusion, direct oblique sagittal CT is easily performed and is complementary to the direct coronal projection for the evaluation of orbital floor and roof fractures. It should not be performed alone.

Optimal evaluation of the orbital floor includes the direct coronal projection with the patient supine and neck hyperflexed and the direct oblique sagittal projection. Optimal evaluation of the orbital roof includes the direct coronal projection with the patient supine and neck hyperextended and the direct oblique sagittal projection.

If only one CT projection is to be used, the direct coronal projection is best. If two CT projections are to be used, a consideration of the frequency distribution of orbital wall fractures should dictate the examination sequence. In addition to being thinner, the floor and medial wall are closer to the central axis of the orbit than the roof and lateral wall and are more often fractured by compression of orbital contents, the probable mechanism of orbital wall blow-out fractures [22]. With this in mind, the initial CT projection should be direct coronal with the patient supine and neck hyperflexed. If an orbital floor fracture is present, the direct oblique sagittal projection can then be obtained. If a medial wall fracture is present, the axial projection can then be obtained. If the orbital floor and medial wall are both involved with fracture, the subsequent projection(s) should be selected on the basis of the need to further evaluate the inferior (direct oblique sagittal projection) or medial (axial projection) rectus muscles. If an orbital roof fracture is present, the direct oblique sagittal projection may be considered for further evaluation. Axial head CT may be prudent to evaluate possible associated intracranial injury.

ACKNOWLEDGMENTS

I thank Robert E. Staton, Judith E. Simon, and Barbara Laxton for help with data collection, and Susan Whisenhunt for text preparation.

REFERENCES

1. Mackenzie W. Traite pratique des maladies des yeux. *Trad Laugier Richelot* (Paris) **1844**;7
2. Lang W. Injuries and disease of the orbit. *Trans Ophthalmol Soc UK* **1889**;9:41–45
3. Smith B, Regan WF Jr. Blow-out fracture of the orbit. *Am J Ophthalmol* **1957**;44:733–739
4. Noyek AM, Kassel EE, Wortzman G, Jazrawy H, Greyson ND, Zizmor J. Contemporary radiologic evaluation in maxillofacial trauma. *Otolaryngol Clin North Am* **1983**;16:473–508
5. Johnson DH Jr. CT of maxillofacial trauma. *Radiol Clin North Am* **1984**;22:131–144
6. Mirsky RG, Saunders RA. A case of isolated medial wall fracture with medial rectus entrapment following seemingly trivial trauma. *J Pediatr Ophthalmol Strabismus* **1979**;16:287–290
7. Curtin HD, Wolfe P, Schramm V. Orbital roof blow-out fractures. *AJNR* **1982**;3:531–534, *AJR* **1982**;139:969–972
8. Ball JB Jr, Towbin RB, Staton RE, Cowdrey KE. Direct sagittal computed tomography of the head. *Radiology* **1985**;155:822
9. Converse JM, Smith B. Enophthalmos and diplopia in fractures of the orbital floor. *Br J Plastic Surg* **1957**;9:265–274
10. Fujino T. Experimental "blowout" fracture of the orbit. *Plast Reconstr Surg* **1974**;54:81–82
11. Putterman AM, Stevens T, Urist MJ. Nonsurgical management of blow-out fractures of the orbital floor. *Am J Ophthalmol* **1974**;77:232–239
12. Koornneef L. Current concepts on the management of orbital blow-out fractures. *Ann Plast Surg* **1982**;9:185–200
13. McLachlan DL, Flanagan JC, Shannon GM. Complications of orbital roof fractures. *Ophthalmology* **1982;**89:1274–1278
14. Cramer LM, Tooze FM, Lerman S. Blowout fractures of the orbit. *Br J Plast Surg* **1965**;18:171–179
15. Gould HR, Titus CO. Internal orbital fractures: the value of laminagraphy in diagnosis. *AJR* **1966**;97:618–623
16. Hammerschlag SB, Hughes S, O'Reilly GV, Naheedy MH, Rumbaugh CL. Blow-out fractures of the orbit: a comparison of computed tomography and conventional radiography with anatomical correlation. *Radiology* **1982**;143:487–492
17. Smith B, Lisman RD, Simonton J, Della Rocca R. Volkmann's contracture of the extraocular muscles following blowout fracture. *Plast Reconstr Surg* **1984**;74:200–216
18. Berkowitz RA, Putterman AM, Patel DB. Prolapse of the globe into the maxillary sinus after orbital floor fracture. *Am J Ophthalmol* **1981**;91:253–257
19. Smith B, Nightingale JD. Fractures of the orbit: blowout and nasoorbital fractures. *Int Ophthalmol Clin* **1978**;18:137–147
20. Stasior OG, Roen JL. Traumatic enophthalmos. *Ophthalmology* **1982**;89:1267–1273
21. Hawes MJ, Dortzbach RK. Surgery on orbital floor fractures: influence of time of repair and fracture size. *Ophthalmology* **1983**;90:1066–1070
22. Jones DEP, Evans JNG. "Blow-out" fractures of the orbit: an investigation into their anatomical basis. *J Laryngol Otol* **1967**;81:1109–1120
23. Yamamoto Y, Sakurai M, Asari S. Towne (half-axial) and semisagittal computed tomography in the evaluation of blow-out fractures of the orbit. *J Comput Assist Tomogr* **1983**;7:306–309